Journal of Mathematical Sciences, Vol. 101, No. 6, 2000

STRESSED STATE OF AN ANISOTROPIC BODY WITH ELLIPTICAL HOLES, ELASTIC INCLUSIONS, AND CRACKS

S. A. Kaloerov, E. S. Goryanskaya, and Yu. B. Shapovalova

UDC 539.3

A method is proposed for studying the two-dimensional stressed state of a multiply connected anisotropic body with cavities and elastic and rigid inclusions, as well as planar cracks and rigid laminar inclusions. Generalized complex potentials, conformal mapping, and the method of least squares are used. The problem is reduced to solving a system of linear algebraic equations. Formulas are given for finding the stress intensity factors in the case of cracks and laminar inclusions. For an anisotropic plate with a single elliptical hole or a crack and an elastic (rigid) inclusion, some numerical results are presented from a study of the effect of the rigidity of the inclusion and the closeness of the contours to one another on the distribution of stresses and the stress intensity factor.

Methods have been proposed [1–3] for determining the two-dimensional stressed state and stress intensity factors for anisotropic bodies with cavities, inclusions, and cracks. These methods are used in the following to study the stressed state of some specific anisotropic bodies with elliptical holes and rigid or elastic inclusions. In the limiting case, elliptical holes and rigid inclusions can change into cracks or rigid laminar inclusions.

We shall consider a cylindrical body-matrix with a general rectilinear anisotropy acted on by external forces and in a two-dimensional stressed state. Let the body be weakened by L longitudinal cavities with elliptical cross sections. The surfaces of J of the cavities are free of support (basic problem I) or are rigidly fastened (basic problem II). Elastic cylindrical inclusions of another anisotropic material are sealed or glued into the remaining $L-J$ cavities in the matrix. The result is a multiply connected region S in the transverse cross section of the body which is bounded by the external contour L_0 and the ellipses $L_l (l = \overline{1, L})$ (Fig. 1), which can be positioned arbitrarily relative to one another, while the others can be transformed into rectilinear cuts. The finite regions corresponding to the elastic inclusions are denoted by $S^l (l = \overline{J+1, L})$. The case where L_0 goes entirely to infinity corresponds to an infinite body with cylindrical cavities and inclusions. We shall assume that the external forces act on the cylindrical surfaces and, for an infinite body, also at infinity in the form of constant stresses σ_x^∞, σ_y^∞, τ_{yz}^∞, τ_{xz}^∞, and τ_{xy}^∞. In the latter case, there is no rotation ω_3^∞ at infinity.

Determining the stressed state of this body reduces to finding the complex potentials $\Phi_k(z_k)$ $(k = \overline{1, 3})$ for the body-matrix and $\Phi_k^{(l)}(z_k^{(l)})$ $(k = \overline{1,3};\ l = \overline{J+1, L})$ for the inclusions from the following boundary conditions at the contours L_l [2, 3]:

$$2\,\mathrm{Re}\sum_{k=1}^{3}\beta_{qkl}\,\delta_{kl}\,\Phi_k'(z_k) = f_{ql}(t)\ \ (q = \overline{1,3}\ \ l = \overline{0,J}) \tag{1}$$

and

$$2\,\mathrm{Re}\sum_{k=1}^{3}\left\{\beta_{qkl}\,\delta_{kl}\,\Phi_k'(z_k) + \beta_{qk}^{(l)}\,\delta_k^{(l)}\,\Phi_k'^{(l)}(z_k^{(l)})\right\} = \varphi_{ql}(t)\ \ (l = \overline{J+1, L};\ q = \overline{1,6}), \tag{2}$$

Donetsk State University. Translated from Teoreticheskaya i Prikladnaya Mekhanika, No. 30, pp. 175–187, 1999. Original article submitted August 10, 1999.

1072-3374/00/1016-3708$25.00 ©2000 Kluwer Academic/Plenum Publishers

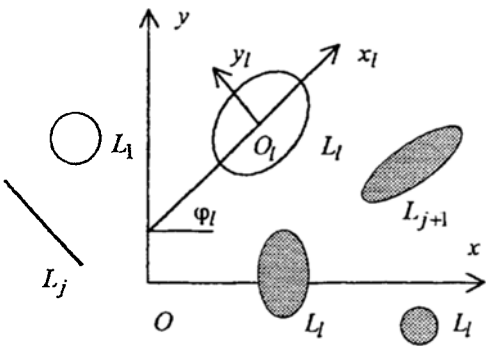

Fig. 1

where [2, 3]

$$\delta_{kl} = -\cos(ny) + \mu_k \cos(nx),\ \delta_k^{(l)} = \cos(ny) - \mu_k^{(l)} \cos(nx); \tag{3}$$

$$\cos nx = y' \Big/ \sqrt{x'^2 + y'^2},\ \cos ny = -x' \Big/ \sqrt{x'^2 + y'^2},$$

$$x'(\theta) = x_l' \cos\varphi_l - y_l' \sin\varphi_l,\ y'(\theta) = x_l' \sin\varphi_l + y_l' \cos\varphi_l;$$

$$x_l' = -a_l \sin\theta,\ y_l' = b_l \cos\theta;$$

μ_k and $\mu_k^{(l)}$ are complex parameters [4] for the matrix and inclusion materials, respectively; a_l and b_l are the semiaxes of the ellipse L_l; θ is the parameter for parametric specification of an ellipse; φ_l is the angle between the positive Ox direction of the main coordinate system and the $O_l x_l$ axis of the local coordinate system associated with ellipse L_l; β_{qkl}, $\beta_{qk}^{(l)}$ and $f_{ql}(t)$, $\varphi_{ql}(t)$ are constants and real functions which depend on the method of loading and supporting the contour L_l.

If the complex potentials have been determined, then the stresses and displacements in the body and in the inclusions can be calculated using the formulas [3, 4]

$$(\sigma_x, \sigma_y, \tau_{yz}, \tau_{xz}, \tau_{xy}) = 2\,\mathrm{Re} \sum_{k=1}^{3} (\lambda_{1k}, \lambda_{2k}, \lambda_{4k}, \lambda_{5k}, \lambda_{6k}) \Phi_k'(z_k),$$

$$\sigma_z = -(a_{13}\sigma_x + a_{23}\sigma_y + a_{34}\tau_{yz} + a_{35}\tau_{xz} + a_{36}\tau_{xy}) / a_{33}; \tag{4}$$

$$(u, v, w) = 2\,\mathrm{Re} \sum_{k=1}^{3} (p_k, q_k, r_k) \Phi_k(z_k) + (-\omega_3 y + u_0,\ \omega_3 x + v_0,\ w_0); \tag{5}$$

$$(\sigma_x^{(l)}, \sigma_y^{(l)}, \tau_{yz}^{(l)}, \tau_{xz}^{(l)}, \tau_{xy}^{(l)}) = 2\,\mathrm{Re} \sum_{k=1}^{3} (\lambda_{1k}^{(l)}, \lambda_{2k}^{(l)}, \lambda_{4k}^{(l)}, \lambda_{5k}^{(l)}, \lambda_{6k}^{(l)}) \Phi_k'^{(l)}(z_k^{(l)}),$$

$$\sigma_z^{(l)} = -(a_{13}^{(l)}\sigma_x^{(l)} + a_{23}^{(l)}\sigma_y^{(l)} + a_{34}^{(l)}\tau_{yz}^{(l)} + a_{35}^{(l)}\tau_{xz}^{(l)} + a_{36}^{(l)}\tau_{xy}^{(l)}) / a_{33}^{(l)}; \tag{6}$$

$$(u^{(l)}, v^{(l)}, w^{(l)}) = 2\,\mathrm{Re} \sum_{k=1}^{3} (p_k^{(l)}, q_k^{(l)}, r_k^{(l)}) \Phi_k^{(l)}(z_k^{(l)}) + (-\omega_3^{(l)} y + u_0^{(l)}, \omega_3^{(l)} x + v_0^{(l)}, w_0^{(l)}). \tag{7}$$

Here

$$\lambda_{1j}=\mu_j^2;\ \lambda_{2j}=1;\ \lambda_{4j}=-\lambda_j;\ \lambda_{5j}=\mu_j\lambda_j;\ \lambda_{6j}=-\mu_j\ \ (j=1,2);$$

$$\lambda_{13}=\mu_3^2\lambda_3;\ \lambda_{23}=\lambda_3;\ \lambda_{43}=-1;\ \lambda_{53}=\mu_3;\ \lambda_{63}=-\mu_3\lambda_3;$$

$$\lambda_{1j}^{(l)}=\mu_j^{(l)^2};\ \lambda_{2j}^{(l)}=1;\ \lambda_{4j}^{(l)}=-\lambda_j^{(l)};\ \lambda_{5j}^{(l)}=\mu_j^{(l)}\lambda_j^{(l)};\ \lambda_{6j}^{(l)}=-\mu_j^{(l)};$$

$$\lambda_{13}^{(l)}=\mu_3^{(l)^2}\lambda_3^{(l)};\ \lambda_{23}^{(l)}=\lambda_3^{(l)};\ \lambda_{43}^{(l)}=-1;\ \lambda_{53}^{(l)}=\mu_3^{(l)};\ \lambda_{63}^{(l)}=-\mu_3^{(l)}\lambda_3^{(l)}; \tag{8}$$

$-\omega_3 y+u_0$, $\omega_3 x+v_0$, and w_0 are the rigid displacements of the matrix; $-\omega_3^{(l)}y+u_0^{(l)}$, $\omega_3^{(l)}x+v_0^{(l)}$, and $w_0^{(l)}$ are the rigid displacements of the lth inclusion as a whole; and p_k, q_k, $p_k^{(l)}$, and $q_k^{(l)}$ are constants that depend on the elastic properties of the matrix and inclusions [2–4].

After suitable conformal mapping, the complex potentials $\Phi_k(z_k)$ and $\Phi_k^{(l)}(z_k^{(l)})$ can be represented by the following series [2, 3]:

$$\Phi_k(z_k)=\Gamma_k z_k+\sum_{l=0}^{L}\sum_{p=1}^{\infty}a_{klp}\varphi_{klp}(z_k),$$

$$\Phi_k^{(l)}(z_k^{(l)})=\sum_{n=0}^{\infty}b_{kn}^{(l)}\psi_{kln}(z_k^{(l)})\quad (l=\overline{J+1,L}), \tag{9}$$

where

$$\varphi_{klp}(z_k)=\begin{cases}\dfrac{z_k^p}{R_{k0}^p} & (l=0),\\[2ex] \dfrac{1}{\zeta_{kl}^p} & (l=\overline{1,L}),\end{cases}$$

$$\psi_{kln}(z_k^{(l)})=\left(\frac{z_k^{(l)}}{R_k^{(l)}}\right)^n; \tag{10}$$

a_{klp} and $b_{kn}^{(l)}$ are unknown constants; ζ_{kl} are variables determined from the implicit dependences [1]

$$z_k=z_{0kl}+R_{kl}(\zeta_{kl}+m_{kl}/\zeta_{kl}),\ z_k^{(l)}=x+\mu_k^{(l)}y, \tag{11}$$

$$R_{kl}=\left[a_l\left(\cos\varphi_l+\mu_k\sin\varphi_l\right)+ib_l\left(\sin\varphi_l-\mu_k\cos\varphi_l\right)\right]/2,$$

$$m_{kl}=\left[a_l\left(\cos\varphi_l+\mu_k\sin\varphi_l\right)-ib_l\left(\sin\varphi_l-\mu_k\cos\varphi_l\right)\right]/2R_{kl},$$

$$z_{0kl}=x_{0l}+\mu_k y_{ol}; \tag{12}$$

and the $R_k^{(l)}$ are constants calculated using a formula obtained from that for R_{kl} by replacing μ_k by $\mu_k^{(l)}$.

Starting with the boundary conditions (1) and (2), we construct the functional

$$I=\sum_{j=1}^{J}\sum_{m=1}^{M_j}\sum_{q=1}^{3}\left|\sum_{k=1}^{3}\left[\beta_{qkj}\delta_{kj}\Phi_k'(z_k)+\overline{\beta}_{qkj}\overline{\delta}_{kj}\,\overline{\Phi_k'(z_k)}\right]-f_{tij}\right|^2+$$

$$+\sum_{j=J+1}^{L}\sum_{m=1}^{M_j}\sum_{q=1}^{6}\left|\sum_{k=1}^{3}[\beta_{qkj}\delta_{kj}\Phi'_k(z_k)+\overline{\beta}_{qkj}\overline{\delta}_{kj}\,\overline{\Phi'_k(z_k)}+\right.$$

$$\left.+\beta^{(j)}_{qk}\delta^{(j)}_{k}\Phi'^{(j)}_{k}(z^{(j)}_{k})+\overline{\beta}^{(j)}_{qk}\overline{\delta}^{(j)}_{k}\overline{\Phi'^{(j)}_{k}(z^{(j)}_{k})}]-\varphi_{qj}\right|^2. \tag{13}$$

Here

$$\Phi'_k(z_k)=\Gamma_k+\sum_{l=0}^{L}\sum_{n=1}^{\infty}a_{kln}\varphi'_{kln}(z_k),$$

$$\Phi'^{(l)}_{k}(z^{(l)}_{k})=\sum_{n=1}^{\infty}b^{(l)}_{kn}\psi'_{kln}(z^{(l)}_{k})\quad(l=\overline{J+1,L}); \tag{14}$$

$$\varphi'_{kln}(z_k)=\begin{cases}\dfrac{nz_k^{n-1}}{R_{k0}^{n}} & (l=0),\\[2ex] -\dfrac{n}{\zeta_{kl}^{n-1}R_{kl}\left(\zeta_{kl}^{2}-m_{kl}\right)} & (l=\overline{1,L}),\end{cases}$$

$$\psi'_{kln}(z^{(l)}_{k})=\frac{n(z^{(l)}_{k})^{n-1}}{(R^{(l)}_{k})^{n}}\quad(l=\overline{J+1,L}). \tag{15}$$

On satisfying the conditions for minimizing the functional (13)

$$\frac{\partial I}{\partial a_{kln}}=0\quad(k=1,2,3;\quad l=\overline{0,L};\quad n=1,2,\ldots);$$

$$\frac{\partial I}{\partial b^{(l)}_{kn}}=0\quad(k=1,2,3;\quad l=\overline{J+1,L};\quad n=1,2,\ldots),$$

we have

$$\sum_{j=1}^{J}\sum_{m=1}^{M_j}\sum_{q=1}^{3}\sum_{s=1}^{3}\beta_{qkj}\delta_{kj}\varphi'_{kln}[\beta_{qsj}\delta_{sj}\Phi'_s(z_s)+\overline{\beta}_{qsj}\overline{\delta}_{sj}\,\overline{\Phi'_s(z_s)}-f_{qj}]+$$

$$+\sum_{j=J+1}^{L}\sum_{m=1}^{M_j}\sum_{q=1}^{6}\sum_{s=1}^{3}\beta_{qkj}\delta_{kj}\varphi'_{kln}\left[\beta_{qsj}\delta_{sj}\Phi'_s(z_s)+\overline{\beta}_{qsj}\overline{\delta}_{sj}\,\overline{\Phi'_s(z_s)}+\right.$$

$$\left.+\beta^{(j)}_{qs}\delta^{(j)}_{s}\Phi'^{(j)}_{s}(z^{(j)}_{s})+\overline{\beta}^{(j)}_{qs}\overline{\delta}^{(j)}_{s}\overline{\Phi'^{(j)}_{s}(z^{(j)}_{s})}-\varphi_{qj}\right]=0\quad(k=\overline{1,3};\quad l=\overline{0,L};\quad n=1,2,\ldots),$$

$$\sum_{j=J+1}^{L}\sum_{m=1}^{M_j}\sum_{q=1}^{6}\sum_{s=1}^{3}\beta^{(j)}_{qk}\delta^{(j)}_{k}\psi'_{kjn}\left[\beta_{qsj}\delta_{sj}\Phi'_s(z_s)+\overline{\beta}_{qsj}\overline{\delta}_{sj}\,\overline{\Phi'_s(z_s)}+\right.$$

$$\left.+\beta^{(j)}_{qs}\delta^{(j)}_{s}\Phi'^{(j)}_{s}(z^{(j)}_{s})+\overline{\beta}^{(j)}_{qs}\overline{\delta}^{(j)}_{s}\overline{\Phi'^{(j)}_{s}(z^{(j)}_{s})}-\varphi_{qj}\right]=0\quad(k=\overline{1,3};\quad n=1,2,3,\ldots). \tag{16}$$

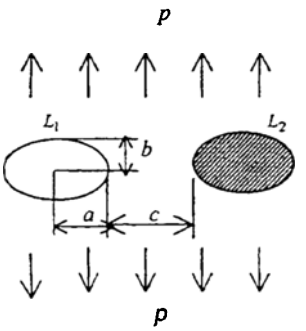

Fig. 2

Substituting Eq. (14) in Eq. (16), we obtain a system of linear algebraic equations for determining the unknown constants a_{kln} and $b_{kn}^{(l)}$:

$$\sum_{j=1}^{J}\sum_{m=1}^{M_j}\sum_{q=1}^{3}\sum_{s=1}^{3}\sum_{r=1}^{L}\sum_{p=1}^{\infty}\beta_{qkj}\delta_{kj}\varphi'_{kln}[\beta_{qsj}\delta_{sj}\varphi'_{srp}a_{srp}+\bar{\beta}_{qsj}\bar{\delta}_{sj}\overline{\varphi'_{srp}}\bar{a}_{srp}]+$$

$$+\sum_{j=J+1}^{L}\sum_{m=1}^{M_j}\sum_{q=1}^{6}\sum_{s=1}^{3}\sum_{r=1}^{L}\sum_{p=1}^{\infty}\beta_{qkj}\delta_{kj}\varphi'_{kln}[\beta_{qsj}\delta_{sj}\varphi'_{srp}a_{srp}+\bar{\beta}_{qsj}\bar{\delta}_{sj}\overline{\varphi'_{srp}}\bar{a}_{srp}+$$

$$+\beta_{qs}^{(j)}\delta_{s}^{(j)}\psi'_{sjp}b_{sp}^{(j)}+\bar{\beta}_{qs}^{(j)}\bar{\delta}_{s}^{(j)}\overline{\psi'_{sjp}}\bar{b}_{sp}^{(j)}]=$$

$$=-\sum_{j=1}^{J}\sum_{m=1}^{M_j}\sum_{q=1}^{3}\sum_{s=1}^{3}\beta_{qkj}\delta_{kj}\varphi'_{kln}[\beta_{qsj}\delta_{sj}\Gamma_s+\bar{\beta}_{qsj}\bar{\delta}_{sj}\bar{\Gamma}_s+f_{qj}]-$$

$$-\sum_{j=J+1}^{L}\sum_{m=1}^{M_j}\sum_{q=1}^{6}\sum_{s=1}^{3}\beta_{qkj}\delta_{kj}\varphi'_{kln}[\beta_{qsj}\delta_{sj}\Gamma_s+\bar{\beta}_{qsj}\bar{\delta}_{sj}\bar{\Gamma}_s+\varphi_{qj}] \tag{17}$$

$$(k=\overline{1,3};\ l=\overline{1,L};\ n=1,2,\ldots).$$

$$\sum_{j=J+1}^{L}\sum_{m=1}^{M_j}\sum_{q=1}^{6}\sum_{s=1}^{3}\sum_{r=1}^{L}\sum_{p=1}^{\infty}\beta_{qk}^{(j)}\delta_{k}^{(j)}\psi'_{kjn}[\beta_{qsj}\delta_{sj}\varphi'_{srp}a_{srp}+$$

$$+\bar{\beta}_{qsj}\bar{\delta}_{sj}\overline{\varphi'_{srp}}\bar{a}_{srp}+\beta_{qs}^{(j)}\delta_{s}^{(j)}\psi'_{sjp}b_{sp}^{(j)}+\bar{\beta}_{qs}^{(j)}\bar{\delta}_{s}^{(j)}\overline{\psi'_{sjp}}\bar{b}_{sp}^{(j)}]=$$

$$=\sum_{j=J+1}^{L}\sum_{m=1}^{M_j}\sum_{q=1}^{6}\sum_{s=1}^{3}\beta_{qk}^{(j)}\delta_{k}^{(j)}\psi'_{kln}[\beta_{qsj}\delta_{sj}\Gamma_s+\bar{\beta}_{qsj}\bar{\delta}_{sj}\bar{\Gamma}_s+\varphi_{qj}]$$

$$(k=\overline{1,3};\ n=1,2,\ldots).$$

Once the last system is solved, the complex potentials are known, so it is possible to compute stresses (4) and (6) on the base areas, as well as the normal and tangential stresses on areas tangential and perpendicular to the contour:

TABLE 1

Stress	θ, deg	λ							
		∞	10	2	0.5	0.1	0.01	0	Rigid incl.
σ_θ^1	0	3.589	3.425	2.758	1.997	1.508	1.353	1.323	0.446
	15	3.201	3.044	2.758	1.991	1.628	1.494	1.486	0.559
	30	2.477	2.333	2.564	1.947	1.803	1.759	1.748	0.683
	45	1.900	1.735	2.166	1.757	1.799	1.831	1.835	0.737
	60	1.353	1.111	1.727	1.326	1.477	1.550	1.574	1.192
	75	–0.144	–0.401	1.159	0.084	0.353	0.458	0.435	2.151
	90	–4.992	–5.540	–5.540	–5.226	–4.996	–4.932	–4.992	0.874
	105	0.383	0.227	–0.051	–0.248	–0.402	–0.459	–0.498	–0.701
	120	1.593	1.534	1.366	1.170	1.045	1.003	0.993	0.183
	135	2.003	1.948	1.813	1.653	1.552	1.518	1.517	0.773
	150	2.292	2.251	2.128	1.981	1.889	1.858	1.852	1.199
	165	2.508	2.462	2.343	2.203	2.114	2.085	2.083	1.483
	180	2.591	2.552	2.433	2.292	2.203	2.175	2.170	1.585
σ_θ^2	0	2.591	2.265	1.522	0.671	0.167	0.027	0.012	–0.060
	15	2.508	2.183	1.459	0.635	0.143	0.036	–0.012	–0.086
	30	2.292	1.961	1.275	0.517	0.063	–0.067	–0.082	–0.172
	45	2.003	1.649	0.979	0.304	–0.066	–0.157	–0.166	–0.316
	60	1.593	1.243	0.599	–0.038	–0.165	–0.145	–0.136	–0.490
	75	0.383	0.366	0.110	–0.075	0.099	0.363	0.414	–0.687
	90	–4.992	–2.904	–0.887	0.358	0.896	1.036	1.052	–0.861
	105	–0.144	0.196	0.097	–0.264	–0.763	–1.109	–1.167	–0.240
	120	1.353	1.236	0.643	–0.006	–0.459	–0.652	–0.680	–0.107
	135	1.900	1.722	1.089	0.419	0.079	–0.127	–0.143	–0.265
	150	2.477	2.204	1.468	0.659	0.149	–0.200	–0.041	–0.285
	165	3.201	2.767	1.872	0.855	0.215	0.005	–0.021	–0.157
	180	3.589	3.047	2.085	0.967	0.269	0.046	0.017	–0.098
σ_r^2	0	0.0	0.064	0.366	0.647	0.703	0.643	0.629	0.636
	15	0.0	0.059	0.369	0.684	0.777	0.732	0.720	0.721
	30	0.0	0.061	0.392	0.790	0.970	0.973	0.969	0.954
	45	0.0	0.089	0.463	0.953	1.239	1.302	1.308	1.271
	60	0.0	0.146	0.590	1.157	1.521	1.632	1.654	1.588
	75	0.0	0.206	0.725	1.345	1.742	1.896	1.884	1.825
	90	0.0	0.235	0.790	1.427	1.819	1.939	1.953	1.937
	105	0.0	0.213	0.735	1.342	1.712	1.822	1.835	1.934
	120	0.0	0.153	0.590	1.159	1.529	1.654	1.669	1.849
	135	0.0	0.104	0.515	1.088	1.508	1.673	1.695	1.490
	150	0.0	0.078	0.488	1.037	1.425	1.576	1.597	0.841
	165	0.0	0.067	0.414	0.807	1.055	1.142	1.153	0.332
	180	0.0	0.065	0.354	0.646	0.818	0.874	0.881	0.121

TABLE 2

θ, deg	c									
	λ = 2					λ = 0.5				
	∞	1	0.5	0.1	0.01	∞	1	0.5	0.1	0.01
					σ_θ^1					
0	2.36	2.55	2.76	3.43	3.86	0.36	2.18	2.00	1.48	1.22
30	2.05	2.13	2.16	2.07	2.00	2.05	1.97	1.95	1.99	2.04
60	1.26	1.25	1.18	0.98	0.90	1.29	1.28	1.33	1.50	1.56
75	–0.12	–0.18	–0.30	–0.52	–0.59	–0.12	–0.04	0.08	0.25	0.32
90	–5.38	–5.44	–5.53	–5.64	–5.65	–5.39	–5.30	–5.23	–5.12	–5.09
105	–0.12	–0.04	0.01	0.11	0.15	–0.12	–0.19	–0.25	–0.32	–0.35
120	1.26	1.32	1.36	1.42	1.44	1.26	1.20	1.17	1.11	1.10
150	2.05	2.10	2.13	2.17	2.18	2.05	2.00	1.98	1.95	1.94
180	2.36	2.41	2.43	2.47	2.48	2.36	2.31	2.29	2.26	2.25
					σ_θ^2					
0	1.39	1.49	1.52	1.57	1.59	0.64	0.66	0.67	0.68	0.69
30	1.10	1.24	1.28	1.33	1.34	0.43	0.51	0.52	0.53	0.54
60	0.52	0.59	0.60	0.62	0.62	0.01	0.05	–0.04	0.04	0.05
75	0.16	0.12	1.10	0.1	0.11	–0.04	–0.03	–0.08	–0.11	–0.12
90	–0.64	–0.75	–0.89	–1.09	–1.15	0.42	0.37	0.36	0.34	0.34
105	0.16	0.24	0.10	–0.17	–0.27	–0.04	–0.23	–0.26	–0.26	–0.25
120	0.52	0.72	0.64	0.44	0.34	0.01	0.01	–0.01	0.03	0.06
150	1.10	1.42	1.47	1.37	1.25	0.43	0.66	0.66	0.62	0.61
180	1.39	1.72	2.09	3.21	3.84	0.64	0.83	0.97	1.17	1.19
					σ_r^2					
0	–0.14	0.31	0.37	0.45	0.48	0.15	0.63	0.65	0.61	0.58
30	0.07	0.36	0.39	0.43	0.44	0.44	0.77	0.79	0.80	0.80
60	0.49	0.58	0.59	0.59	0.59	1.00	1.15	1.16	1.17	1.17
75	0.64	0.71	0.73	0.74	0.74	1.21	1.33	1.35	1.36	1.36
90	0.94	0.77	0.79	0.82	0.83	1.28	1.40	1.43	1.45	1.46
105	0.64	0.70	0.74	0.78	0.80	1.21	1.30	1.34	1.39	1.40
120	0.49	0.55	0.60	0.67	0.70	1.00	1.09	1.16	1.26	1.30
150	0.07	0.40	0.49	0.66	0.75	0.44	0.91	1.04	1.25	1.32
180	–0.14	0.38	0.35	0.12	–0.04	0.15	0.80	0.65	0.21	0.04

$$\sigma_n = \sigma_x \cos^2 nx + \sigma_y \cos^2 ny + 2\tau_{xy} \cos nx \cos ny,$$

$$\sigma_s = \sigma_x \cos^2 ny + \sigma_y \cos^2 nx - 2\tau_{xy} \cos nx \cos ny,$$

$$\tau_{nz} = \tau_{yz} \cos ny + \tau_{xz} \cos nx, \quad \tau_{sz} = \tau_{yz} \cos nx - \tau_{xz} \cos ny,$$

$$\tau_{ns} = (\sigma_y - \sigma_x) \cos nx \cos ny + \tau_{xy} (\cos^2 nx - \cos^2 ny). \tag{18}$$

The analogous stresses on the lth inclusion are

$$\sigma_n^{(l)} = \sigma_x^{(l)} \cos^2 nx + \sigma_y^{(l)} \cos^2 ny + 2\tau_{xy}^{(l)} \cos nx \cos ny,$$

TABLE 3

θ, deg	b/a				
	1	0.5	0.1	0.05	0.01
			σ_θ^1		
0	2.00	3.30	5.14	9.79	49.86
15	1.99	2.95	–0.03	–2.05	–6.55
30	1.95	2.26	0.04	–1.33	–2.23
45	1.76	1.25	1.76	2.16	1.84
60	1.33	1.26	2.48	2.78	3.01
90	–5.23	–4.99	–1.63	–0.76	–0.37
120	1.17	0.51	–3.88	–3.97	–3.54
135	1.65	1.78	–2.42	–4.08	–4.87
150	1.98	2.50	0.98	–1.98	–5.41
165	2.20	3.14	5.50	5.12	–3.08
180	2.29	3.54	10.87	19.78	91.42
			σ_θ^2		
0	0.67	0.65	0.65	0.65	0.64
30	0.52	0.52	0.44	0.43	0.43
60	–0.04	–0.02	0.00	0.00	0.00
75	–0.08	–0.22	–0.02	–0.02	–0.04
90	0.39	0.31	0.44	0.44	0.44
105	–0.26	–0.28	–0.19	–0.14	–0.08
120	–0.01	–0.31	–0.11	–0.07	–0.05
135	0.42	–0.05	0.12	0.14	0.16
150	0.66	0.46	0.38	0.38	0.40
165	0.86	0.88	0.60	0.59	0.59
180	0.97	0.97	0.67	0.67	0.67
			σ_r^2		
0	0.65	0.69	0.15	0.15	0.15
30	0.79	0.60	0.44	0.44	0.44
60	1.16	1.04	1.03	1.02	1.02
75	1.35	1.28	1.25	1.24	1.24
90	1.43	1.39	1.33	1.32	1.32
105	1.34	1.33	1.27	1.26	1.26
120	1.16	1.08	1.06	1.06	1.06
135	1.09	0.65	0.76	0.77	0.77
150	1.04	0.36	0.44	0.46	0.47
165	0.81	0.95	0.31	0.28	0.25
180	0.65	1.43	0.60	0.41	0.25

$$\sigma_s^{(l)} = \sigma_x^{(l)} \cos^2 ny + \sigma_y^{(l)} \cos^2 nx - 2\tau_{xy}^{(l)} \cos nx \cos ny,$$

$$\tau_{nz}^{(l)} = \tau_{yz}^{(l)} \cos ny + \tau_{xz}^{(l)\nu} \cos nx, \quad \tau_{sz}^{(l)} = \tau_{yz}^{(l)} \cos nx - \tau_{xz}^{(l)} \cos ny,$$

$$\tau_{ns}^{(l)} = (\sigma_y^{(l)} - \sigma_x^{(l)}) \cos nx \cos ny + \tau_{xy}^{(l)} (\cos^2 nx - \cos^2 ny). \tag{19}$$

TABLE 4

	θ, deg	ε							
		$\lambda = 2$				$\lambda = 0.5$			
		∞	0.5	0.1	0.01	∞	0.5	0.1	0.01
σ_θ^2	0	1.39	1.34	1.27	1.28	0.64	0.64	0.63	0.63
	30	1.10	1.06	0.98	0.99	0.43	0.43	0.42	0.42
	60	0.52	0.47	0.37	0.39	0.01	0.00	0.01	0.01
	75	0.16	0.12	0.04	–0.01	–0.04	–0.05	–0.01	0.00
	90	–0.65	–0.53	–0.38	–0.41	0.42	0.44	0.44	0.48
	105	0.16	0.13	0.27	0.29	–0.04	–0.08	–0.08	–0.12
	120	0.52	0.44	0.49	0.49	0.01	–0.04	–0.04	–0.05
	135	0.82	0.72	0.71	0.72	0.21	0.16	0.16	0.15
	150	1.10	0.99	0.91	0.94	0.43	0.40	0.40	0.38
	165	1.31	1.23	0.83	0.90	0.59	0.59	0.59	0.51
	180	1.39	1.33	0.45	0.26	0.64	0.67	0.67	0.48
σ_r^2	0	–0.14	–0.12	–0.09	–0.09	0.15	0.16	0.12	0.11
	30	0.07	0.09	0.12	0.12	0.43	0.44	0.43	0.43
	60	0.49	0.53	0.57	0.56	1.00	1.02	1.02	1.02
	75	0.64	0.70	0.76	0.76	1.21	1.23	1.24	1.24
	90	0.69	0.78	0.83	0.82	1.28	1.32	1.32	1.32
	105	0.64	0.74	0.82	0.83	1.21	1.26	1.26	1.26
	120	0.49	0.60	0.68	0.66	1.00	1.06	1.06	1.05
	135	0.27	0.39	0.51	0.52	0.72	0.77	0.78	0.79
	150	0.07	0.15	0.28	0.26	0.43	0.47	0.48	0.49
	165	–0.08	–0.03	0.18	0.19	0.23	0.25	0.30	0.31
	180	–0.14	–0.03	0.29	0.66	0.15	0.23	0.39	0.85
K_1^+		1.00	0.68	0.59	0.55	1.00	0.65	0.58	0.58
K_1^-		1.00	0.45	0.07	0.03	1.00	0.37	0.04	0.03

If some of the contours L_l degenerate into a rectilinear cut or a rigid linear inclusion, then it is possible to calculate the stress intensity factors near the ends of the corresponding planar crack or laminar rigid inclusion [5]:

$$K_1 = \lim_{r\to 0} \sqrt{2r}(\sigma_x \sin^2\varphi_l + \sigma_y \cos^2\varphi_l - 2\tau_{xy}\cos\varphi_l \sin\varphi_l),$$

$$K_2 = \lim_{r\to 0} \sqrt{2r}[(\sigma_y - \sigma_x)\sin\varphi_l \cos\varphi_l + 2\tau_{xy}(\cos^2\varphi_l - \sin^2\varphi_l)],$$

$$K_3 = \lim_{r\to 0} \sqrt{2r}(\tau_{yz}\cos\varphi_l - \tau_{xz}\sin\varphi_l). \tag{20}$$

Some numerical studies were done of the stress distribution and the changes in the stress intensity factors for an anisotropic plate with an elliptical elastic inclusion in the presence of an elliptical hole which can degenerate into a crack or an absolutely rigid rectilinear inclusion. The plate was acted on by stresses $\sigma_y^\infty = p$ (Fig. 2). In this case, the subscript k in all the formulas given above takes the values 1 or 2, while all quantities for $k = 3$ equal zero. Here [3] we have

$$L = 2; \quad (\beta_{1kj}, \beta_{2kj}) = (\lambda_{6k}, \lambda_{2k}) \quad (j = 1, 2); \quad (\beta_{4k2}, \beta_{5k2}) = (p_k, q_k).$$

$$(\beta_{1k}^{(2)}, \beta_{2k}^{(2)}, \beta_{4k}^{(2)}, \beta_{5k}^{(2)}) = (\lambda_{6k}^{(2)}, \lambda_{2k}^{(2)}, -p_k^{(2)}, -q_k^{(2)}),$$

$$f_{q1} = 0, \quad \varphi_{q2} = 0.$$

The plate material was taken to be fiberglass, for which $a_{11} = 6.711$, $a_{12} = 2.081$, $a_{13} = a_{16} = a_{26} = 0.000$, $a_{22} = 166.670$, $a_{66} = 250.00$, $\mu_1 = 0.831i$, $\mu_2 = 6.481i$. The core material was assumed to be a material for which the deformation coefficients are calculated using the formulas $a_{ij}^{(2)} = \lambda a_{ij}$.

The normal stresses σ_θ^1 in the plate near an unsupported contour L_1, σ_θ^2 near a contour L_2 on areas perpendicular to the contours, and the normal stresses σ_r^2 on areas tangential to the contour of an inclusion are given in the following tables.

For various values of the parameter λ, Table 1 lists the stresses σ_θ^1, σ_θ^2, and σ_r^2 for contours L_1 and L_2 that are circles with the same radius separated by a distance $c = 0.5$. Here λ equal to ∞ and 0 corresponds to the cases of absolutely flexible (a plate with two circular holes) and absolutely rigid (plate with a circular hole and a rigid core) inclusions. The data of Table 1 show that as the rigidity of the core increases (as λ is reduced), σ_θ^1 and σ_θ^2 decrease near the hole and the inclusion, while σ_r^2 increases.

For different values of c, Table 2 lists the stresses σ_θ^1, σ_θ^2, and σ_r^2 near circular contours L_1 and L_2 with the same radius. These data show that on approaching a hole with an inclusion, σ_θ^1 near the contour of the hole increases for $\lambda > 1$ and decreases for $\lambda < 1$, while σ_θ^2 and σ_r^2 near the contour of an inclusion increase for arbitrary λ. An especially high stress concentration is seen in the zone between the contours.

Table 3 lists the stresses σ_θ^1, σ_θ^2, and σ_r^2 as functions of half axis b of the contour L_1. Here the half axis a of the contour L_1 and the radius of the circular inclusion L_2 were equal to 1. It was also assumed that $\lambda = 2$ and $c = 0.5$. Table 3 shows that as $b \to 0$, there is a sharp rise in the stress concentration near the ends of the diameter $2a$ of contour L_1. Here the stresses near the contour of inclusion L_2 vary little. As the calculations show, for $b \le 10^{-3}$, the ellipse L_1 can be regarded as a rectilinear crack.

Table 4 lists the stresses σ_θ^2 and σ_r^2, as well as the stress intensity factors for the ends of the crack in a plate with a crack L_1 of half length 1 and a circular inclusion L_2 of unit radius. These data show that on approaching a crack with an elastic inclusion, the stress intensity factors vary significantly, while the stresses vary little.

REFERENCES

1. S. A. Kaloerov and E. S. Goryanskaya, "Two-dimensional stressed state of a multiply connected anisotropic body with cavities and cracks," *Teor. Prikl. Mekh.*, No. 25, 45–56 (1997).
2. S. A. Kaloerov and E. S. Goryanskaya, "Two-dimensional stressed-deformed state of a multiply connected anisotropic body," in: A. N. Guz' et al. (eds.), *Stress Concentration* [in Russian], Vol. 7 of *The Mechanics of Composites* in 12 vols., Kiev (1998), pp. 10–26.
3. S. A. Kaloerov, E. S. Goryanskaya, and Yu. B. Shapovalova, "Two-dimensional stressed-deformed state of an anisotropic body with holes, elastic inclusions, and cracks," *Teor. Prikl. Mekh.*, No. 29, 63–70 (1999).
4. S. G. Lekhnitskii, *Theory of Elasticity of Anisotropic Bodies* [in Russian], Moscow (1977).
5. S. A. Kaloerov, "Approximate method for determining stress intensity factors for two-dimensional multiply connected bodies with rectilinear cracks," *Teor. Prikl. Mekh.*, No. 24, 27–33 (1993).